

SUPPLEMENTAL MATERIAL

SUPPLEMENTAL METHODS

Mice

TMEM43WT and TMEM43mut mice, in the C57BL/6JCrI (Charles River Laboratories) background, respectively express human wild type TMEM43 and human TMEM43-S358L specifically in cardiomyocytes under the control of the α -myosin heavy chain (MHC) promoter. Wild type C57BL/6 JCrI mice were used as controls. TMEM43mut male mice were crossed with α MHC-CnA β 1 mice¹ to generate the double transgenic mouse line TMEM43mut-CnA β 1. Male and female mice were used throughout the study. Mice were housed in an air-conditioned room with a 12h light/dark cycle and free access to water and chow. For the inhibition of galectin 3, GM-CT-01 was used. TMEM43mut mice were randomized to the saline-treated control group (n=8) or the GM-CT-01-treated group (n=8). Mice were treated twice a week with intravenous injections of GM-CT-01 (120 mg/kg) or placebo (normal saline) in the tail vein from 5 weeks of age until 4 months. For GSK3 inhibition, mice were injected i.p. daily with SB216763 (2.5 mg/kg/day). Animals were randomly assigned to groups (block randomization). Researchers were blinded to the allocations. Power calculations were carried out to determine the necessary number of animals based on prior data (p=0.05; power=80%). All procedures were approved by the CNIC Ethics Committee and the Regional Government of Madrid. All animal experiments conformed to EU Directive 2010/63EU and Recommendation 2007/526/EC, enforced in Spanish law under Real Decreto 53/2013.

Echocardiography

Cardiac function, chamber dilatation, and wall thickness were analyzed in neonatal mice and in mice aged 3 and 5 weeks and 2 and 4 months by transthoracic two-dimensional (2D), and M-mode (MM) echocardiography. Measurements were carried out by a blinded operator using a high-frequency ultrasound system with a 50-MHz linear probe for

neonates and a 30-MHz probe for older mice (Vevo 2100, Visualsonics Inc., Canada). For ultrasound scans, mice were placed on a heating pad; neonates were not anesthetized, whereas older mice were kept under light anesthesia with isoflurane adjusted to obtain a target heart rate of 500 ± 50 bpm. Left ventricular (LV) ejection fraction (LVEF) and LV end-diastolic volume (LVEDV) were obtained from the long axis view, and LV posterior wall in diastole (LVPWd) from the short axis view. Right ventricular (RV) systolic function was assessed indirectly from the tricuspid annular plane systolic excursion (TAPSE), estimated from maximum lateral tricuspid annulus movement obtained from a 2D 4-chamber apical view. Images were analyzed off-line by a blinded expert using the Vevo 2100 Workstation software. Animals were sacrificed by gradually filling the chamber with carbon dioxide. Mice and hearts and lungs were weighed after sacrifice.

Electrocardiograms (ECGs)

ECGs were obtained in unanesthetized neonates and in 3- and 5-week-old and 2- and 4-month-old anesthetized mice by using bipolar limb leads (leads I, II, and III) and unipolar limb leads (leads aVR, aVL, and aVF) for 60-90 seconds. Measurements were taken by a blinded operator with mice (except for neonates) placed under light anesthesia with isoflurane (MP36R, BIOPAC Systems, Inc.). ECGs were analyzed by an expert using Acqknowledge 4.1.1. for MP36R (BIOPAC Systems, Inc.). Mean values were calculated from 10 consecutive standard ECG time intervals and waves.

Lineage tracing

We generated four sets of lineage tracing mice using *Cre-LoxP* technology to enable us to track the fate of different cell populations and their contribution to fibrotic replacement. Each line carried a floxed reporter allele (*EYFP*, *RFP*, or *GFP*) preceded by a STOP codon that was removed upon recombination by the Cre recombinase. Each Cre recombinase was regulated by lineage-specific promoters. Cre-expressing cells and

their progeny were permanently labeled by expression of the reporter. We used this method to determine the contribution of the endothelial (*Tie2-Cre*)², macrophage (*LysM-Cre*)³, epicardial (*Wt1-Cre*)⁴, and cardiomyocyte (*cTnT-Cre*)⁵ lineages. Each of these mouse lines was crossed with transgenic TMEM43mut mice in order to analyze the contribution of each cell lineage to the fibroblast fate. Mature collagen fibers in the myocardium were visualized by second harmonic generation microscopy⁶. General tissue fibrosis was detected by confocal reflection microscopy⁷.

Histological analysis, immunohistochemistry, and immunofluorescence

Samples were fixed in paraformaldehyde (4% in PBS) for 48h, washed in PBS, dehydrated, and included in paraffin. Five-micron thick sections were rehydrated and stained. The extracellular matrix content of the hearts was analyzed using Masson's trichrome protocol⁸. Collagen fiber content, hue, and spatial distribution were assessed by Picrosirius Red staining⁷. For each staining, we analyzed three independent 20x microscope fields from the right and left ventricles and the interventricular septum in neonatal mice and in 5-week-old and 2- and 4-month-old mice using Fiji⁹.

Paraffin sections were deparaffinized and rehydrated before heat-induced epitope retrieval (HIER) with citrate buffer (pH 6.0). Sections were then washed with 0.1% Tween 20 in PBS, blocked in 10% goat serum/PBS 0.1% Tween for 30 min at room temperature, and incubated in 1% goat serum/PBS overnight at 4°C with the appropriate antibody: anti-TMEM43 (1:50 ab184164 from Abcam, sc-365298 from Santa Cruz and guinea pig anti-TMEM43 kindly provided by Dr. Franke, Heidelberg Germany), anti-Connexin 43 (1:500; c6219, Sigma), anti-GFP (1:100; NB100-1614-0.02ml, Novus Biologicals), or anti-RFP (1:200; 600-401-379, Rockland). After primary antibody incubation, sections were washed with PBS, incubated with Alexa Fluor 564 goat anti-chicken IgY (A-11040; Life Technologies) or Alexa Fluor 647 goat anti-rabbit IgG (A-21244 ; Life Technologies) in 1% goat serum/PBS for 1 h at room temperature, and

mounted in Vectashield mounting medium (Vector Laboratories, Burlingame, California). Nuclear DNA was stained with either DAPI (1:1000) or To-Pro-3 Iodide (1:10.000; T3605, Life Technologies).

Immunohistochemistry followed almost the same protocol, with goat-serum incubation preceded by blocking with Avidin/Biotin Blocking Kit according to the manufacturer's protocol (Vector Laboratories, Burlingame, California). Primary and secondary antibodies used included perilipin (9349, Cell Signaling) and anti-rabbit-HRP (P044801-2, Dako). The Vectastain ABC kit was used to amplify the signal, and the DAB substrate kit was used for peroxidase detection, according to the manufacturer's instructions (Vector Laboratories, Burlingame, California). Counterstaining with hematoxylin was carried out before dehydration and mounting in DPX.

Immunofluorescence images were acquired with a Nikon A1R multi-line inverted confocal microscope, a Plan Apo VC 60x/1,4 Oil DIC N2 Oil objective, and Nikon NIS reprocessing software. For lineage tracing, images were acquired with a multiphoton Zeiss LSM 780 confocal microscope, a W Plan-Apochromat 20x/1,0 DIC M27 75mm WD 1.8 mm objective, and Zeiss ZEN reprocessing software. Images for immunohistochemistry were digitalized with a NanoZoomer-2.0RS® (Hamamatsu). All images were analyzed off-line with Fiji⁹, and brightness and contrast were linearly adjusted using Adobe Photoshop CS5.1.

Cell culture, transfection, and immunofluorescence

P19 cells were transfected with the following HA-tagged expression vectors for TMEM43: TMEM43WT-Ct-HA, Nt-HA-TMEM43WT, TMEM43-S358L-Ct-HA, and Nt-HA-TMEM43-S358L, where Nt and Ct indicate attachment of the HA tag to the N-terminus or the C-terminus. Cells were fixed in 4% PFA in PBS for 10 min at 4°C, permeabilized for 10 min with 0.1% Triton X-100/PBS, and incubated in 10% goat serum/PBS for 30 min at room temperature. Cells were incubated overnight in 1% goat serum/PBS with anti-HA

(11583816001, Roche). After primary antibody incubation, cells were washed with PBS, incubated for 1 h at room temperature with Alexa Fluor 488 goat anti-mouse IgG (A-11029; Thermo Fischer Scientific) and DAPI in 1% goat serum/PBS, and mounted in Vectashield mounting medium. Images were acquired with a Nikon A1R multi-line inverted confocal microscope, a Plan Apo VC 60x/1,4 Oil DIC N2 Oil objective, and Nikon NIS reprocessing software. Brightness and contrast were linearly adjusted using Adobe Photoshop CS5.1.

Luciferase assay

Cardiomyocytes were transfected as described above with pcDNA3.1 expression vectors for the different TMEM43 constructs or containing CnA β 1 and the TCF-Luc reporter plasmid, in which luciferase expression is under the control of a TCF binding site multimer, which in turn is activated by β -catenin. Where indicated, cells were treated with 3 μ m CHIR99021 (SML1046-5MG, Sigma). A reporter plasmid expressing Renilla luciferase was cotransfected for normalization. Cells were lysed in 1x passive lysis buffer (E1910, Promega) and homogenized for 15 min at room temperature. Luciferase was measured according to the manufacturer's instructions (E1910, Promega) and normalized for transfection efficiency with Renilla luciferase.

Cell viability assay

P19 cells were transfected with pcDNA3.1 expression vectors for the different TMEM43 constructs as described above and grown overnight in the presence of 10% fetal calf serum (FCS). FCS was then removed and cell viability was determined 32 h later using propidium iodide. Where indicated, cells were treated with 3 μ m CHIR99021. Control cells were incubated with 10% ethanol for 5h for cell death monitoring.

Western blot

Hearts were homogenized in lysis buffer (150 mM NaCl, 1% IGEPAL, 0.5% sodium deoxycholate, 0.1% SDS, and 50 mM Tris [pH 8.0]) in the presence of protease and phosphatase inhibitors (5892791001 and 04906845001, respectively, from Roche). Samples were sonicated, and lysates were separated in SDS-PAGE gels, transferred to polyvinylidene fluoride (PVDF) membranes, and blocked with 3% non-fat dry milk in PBS for 30 min. The membranes were incubated with primary antibodies overnight, followed by appropriate horseradish peroxidase (HRP)-labeled secondary antibodies (anti-goat P044901, anti-mouse P044701, and anti-rabbit P044801-2, Dako). HRP activity was detected using a luminol-based detection reagent (GERPN2209, SIGMA and RPN2232, GE Healthcare). Primary antibodies were as follows: TMEM43 (ab184164, Abcam and sc-365298, Santa Cruz), GSK3 β (9315; Cell Signaling), p-GSK3b (9323; Cell Signaling), galectin-3 (CL8942AP, Cedarlane), β -actin (A5316; Sigma), emerin (EMD, ab125494, Abcam), AKT (9272, Cell Signaling), phospho-AKT Ser473 (9271, Cell Signaling), active caspase-3 (9661; Cell Signaling), pro-caspase-3 (9662; Cell Signaling), beclin 1 (3738; Cell Signaling), GAPDH (ab75834, Abcam), vinculin (V4505; Sigma). Brightness and contrast were linearly adjusted in Adobe Photoshop CS5 and western blots were quantified with Image Studio Lite (LI-COR Biosciences).

Immunoprecipitation

TMEM43 immunoprecipitation experiments were performed in the P19 cell line. Briefly, cells were transfected as described above. Cells were lysed with TBS buffer (150 mM NaCl, 20 mM Tris-HCl pH 7.4) supplemented with 1% Nonidet P-40, 5 mM EDTA, 5 mM MgCl₂, and 1 \times complete protease, phosphatase, and acetylase inhibitors. Protein extracts were incubated with anti-HA–conjugated Dynabeads (Life Technologies) for 1 h at 4°C. Beads were washed three times with lysis buffer containing 0.05% Nonidet P-40 and 5 times with lysis buffer without added detergent. Bound proteins were released from beads by boiling in 4 \times Laemmli sample buffer. Immunoprecipitates and input samples

were resolved by SDS-PAGE or subjected to protein digestion followed by nanoliquid chromatography coupled to mass spectrometry for protein identification and quantification by peptide counting¹⁰. The proteomics dataset (raw and msf files and protein database) is available in the PeptideAtlas repository (<http://www.peptideatlas.org/PASS/PASS01063>), which can be downloaded via [ftp.peptideatlas.org](ftp://ftp.peptideatlas.org): username, PASS01063; password, FZ6532b.

RNA isolation and qRT-PCR

After sacrificing the animals, mice were perfused with PBS, hearts were excised, and samples from the different heart chambers were separated and snap-frozen in liquid nitrogen. Total RNA was isolated from mouse hearts with TRIzol reagent (15596026, Thermo Fischer Scientific). First-strand cDNA was synthesized using 100 ng of total RNA and a High Capacity cDNA Reverse Transcription Kit (4368814, Thermo Fischer Scientific). Quantitative reverse-transcribed real-time PCR (qRT-PCR) was carried out using SYBER green and the following primers: Acta1 forward 5'-GACCACAGCTGAACGTGAGA-3', Acta1 reverse: 5'-TGTTGTAGGTGGTCTCATGGAT-3', Col1 α 1 forward: 5'-GTGCCACTCTGACTGGAAGA-3', Col1 α 1 reverse: 5'-CTGACCTGTCTCCATGTTGC-3', Lgals3 forward: 5'-ATGCTGATCACAATCATGGG-3', Lgals3 reverse: 5'-GCAACATCATTCCCTCTCCT-3', Lox forward: 5'-GCTGCGGAAGAAAAGTGC-3', Lox reverse: 5'-CCTTGTTTCTTCACTCTTTGC-3', Nppa forward: 5'-GATGGATTTCAAGAACCTGCT-3', Nppb forward: 5'-GCCAGTCTCCAGAGCAATTC-3', Nppb reverse: 5'-TCTTTTGTGAGGCCTTGGTC-3', TMEM43 forward: 5'-TGACACGGATCCTCTACACCT-3', TMEM43 reverse: 5'-TTGGAGTGAAAAGACCCTGG-3'. Gene expression was normalized to Gapdh. qRT-PCR was carried out in an ABI PRISM® 7900HT FAST Real-Time PCR System (Applied Biosystems) using SYBR green for double-stranded DNA detection. Results were analyzed with LinReg PCR software¹¹.

RNA sequencing and analysis

Total RNA was extracted from the right ventricles of 2-month-old WT, TMEM43WT, and TMEM43mut mice (n=3 for each mouse line) as described above. 500 ng of total RNA were used to generate barcoded RNA-seq libraries using the TruSeq RNA sample preparation kit (Illumina) after poly A+ RNA selection using polyT oligo-attached magnetic beads with two rounds of purification followed by fragmentation and first and second cDNA strand synthesis. Next, cDNA ends were repaired and adenylated, and the adapters were ligated, followed by PCR library amplification. Finally, library size was checked with an Agilent 2100 Bioanalyzer DNA 1000 chip, and concentrations were determined in a Qubit® fluorometer (Life Technologies). Libraries were sequenced on a HiSeq2500 (Illumina) to generate 60-base single reads. FastQ files for each sample were obtained with CASAVA v1.8 (Illumina). An average of 22 M reads were obtained per sample (93% mapped). For each of the comparisons we considered genes to be differentially expressed when the adjusted p-value was lower than 0.05 and absolute log(Fold Change) was higher than 0.5. We then used the Webgestalt online tool (<http://www.webgestalt.org/option.php>) to identify over-represented Gene Ontology (GO) terms in this reduced list of genes, using as a background the whole set of genes detected in the experiment. We selected the 10 most significantly enriched categories and 100 genes with highest absolute log(Fold Change) and represented them in a Circos plot using GOplot (<http://wencke.github.io/>)¹². Alternative splicing analysis was performed using vast-tools v0.2.0. Events were considered to be differentially spliced whenever the posterior probability of having a difference between the two conditions higher than 0 was higher than 0.95¹³⁻¹⁵. RNA-Seq data are available in the public GEO repository database with the accession number GSE101301 (<https://www.ncbi.nlm.nih.gov/geo/query/acc.cgi?acc=GSE101301>).

In silico modeling and docking of TMEM43

Fasta sequences of WT TMEM43 and TMEM43-S358L (UniProt ID: Q9BTV4) and EMD (Uniprot ID P50402) were analyzed with a local implementation of Rosetta software suite v3.5 (www.rosettacommons.org)¹⁶ for ab-initio modeling using the mp_framework of the suite. In each case, the models obtained before were clustered using the cluster tool and filtered by correct topology. The lowest energy model was selected in each case and a final refinement step was made using the Modrefiner tool from a local implementation of iTasser v4.1 suite¹⁷.

Final models for the obtained monomers were positioned according to the dimeric interface using pymol v1.7.1 (The PyMOL Molecular Graphics System, Version 1.7.1 Open Source, Schrödinger, LLC. www.pymol.org), and each new dimeric model was used as the initial template. For each template, a span file with coordinates for the theoretical membrane domain was computed using the mp_span_from_pdb tool from the membrane framework of Rosetta suite v3.5. Using the obtained complex templates, a cycle of docking with positional restrictions (docking interface by TM1) was carried out for each dimer using the *mp_dock* application¹⁸ from the membrane framework of the Rosetta suite and structural clustering. The final selected model in each case was the lowest scoring refined model (lower E) with correct topology and interface. A similar protocol was used for complexes of TMEM43 homodimers or heterodimers (WT:mut) with EMD.

Human induced pluripotent stem cells-derived cardiomyocytes (hiPSC-CMs)

The *TMEM43*^{C1073T} mutation was introduced in the *TMEM43* allele of a WT hiPSC line (HDF-iPS-SV10) by using CRISPR-Cas9 technology. The specific sequence for crRNAs was designed using CRISPOR-TEFOR software (<http://crispor.tefor.net/crispor.py>), selecting the crRNA sequence with the least off-targets and highest efficiency, surrounding the nucleotide of the intended mutation. ssODN was designed to insert the intended mutation (bold) and silent variants avoiding subsequent recognition of the crRNA and allowing RE digestion (EagI, grey) for genotyping. The following primers were

used: crRNA: 5'-ACCCTGCTGACCGTGGCGGC-3'; ssODN: 5'-TTCCGAGACCTGGTAAACATAGGCCTGAAAGCCTTTGCCTTCTGTGTGGCCACCTTGCTGACACTCCTCACAGTGGCGGCCGGCTGGCTCTTCTACCGACCCCTGTGGGCCCTCCTCATTGCCGGCCTGGCCCTTGTGCCCATCCTTGTTGCT-3';

hTMEM43_Fwd: 5'- GAATGAACCAACACCTCTAGGAAT-3'; hTMEM43_Rev: 5'-AGTCCAAGAGAGGAAGGAAACAG-3'. Synthetic crRNA and tracrRNA (AltR CRISPR-Cas9 system, IDT) were mixed in equimolar concentrations and 2.2 pmol/each were combined with 25 μ M Cas9 Nuclease 3NLS to form the ribonucleoprotein (RNP) complex. The RNA complex plus ssODN and AltR Cas9 Electroporator Enhancer (1075915, IDT) (22 pmol/each) were electroporated into HDF-iPS-SV10 (2.5×10^5) using Neon Transfection System and Neon Transfection System Kit 10 μ l (Thermo Fisher) following supplier instructions. 1400 V/ 20 ms/1 pulse was applied. Cells were recovered in Essential E8 medium (Thermo Fisher) plus ROCK inhibitor (Stem MACS Y-27632 Miltenyi) and plated into a p48 well. After 48 h, cells were split into 4 p100 dishes at a density of 5×10^3 cells/p100. After 7-10 days, a total of 172 clones were picked up for screening. DNA from clones was isolated, PCR amplified and EagI digested. Two clones were identified as positive and were Sanger sequenced. One of the clones was confirmed to carry the desired mutation.

For cardiac differentiation, cells were maintained on Matrigel-coated plates in Essential E8 medium (Thermo Fisher), dissociated into single cells with Accutase (Thermo Fisher) at 37°C for 8 min and seeded onto Matrigel-coated 12-well plate at a density of $1-1.5 \times 10^6$ cells per well in Essential E8 medium supplemented with 10 μ M ROCK inhibitor (day -3). Medium was changed daily for 3 days. When hiPSC achieved confluence, cells were treated with a GSK3 inhibitor (CHIR99021, Stemgent) (*WT* hiPSC 8 μ M, and *TMEM43*^{C1073T} 4 μ M) in RPMI (Thermo Fisher) supplemented with B27 lacking insulin (Thermo Fisher) for 24 h (day 0 to day 1). After 24 h, the medium was changed to RPMI/B27-insulin and cultured for another 2 days. On day 3, cells were treated with 5

μ M Wnt inhibitor IWP4 (Stemgent) in RPMI/B27-insulin medium and cultured for 4 days, changing medium every 2 day. Cells were maintained in RPMI supplemented with B27 (Thermo Fisher), (RPMI/B27 medium) starting from day 7, with medium change every 2-3 days. On day 10-12, contracting cardiomyocytes were obtained¹⁹.

For iPSC-derived cardiac monolayer maturation, cells were disaggregated at d15 and seeded onto Matrigel-coated PDMS membranes as described²⁰. *WT* and *TMEM43*^{C1073T} hiPSC were maintained in RPMI/B27 medium for 1 week for further maturation, and disaggregated (at day 20 and at day 32) by incubation with 0.25% trypsin-EDTA (Thermo Fisher) for 5 min at 37 °C for in vitro studies. hiPSC-CM were treated with the GSK3 inhibitor CHIR99021 (4 μ M) or DMSO as a control vehicle. Video recording was taken 2 after treatment. hiPSC-CM contraction was measured using the Musclemotion algorithm, as described²¹.

For calcium measurements, hiPSC-CMs were loaded for 30 min. with 5 μ M Fluo 4-AM and 0.02% pluronic F127 in culture medium at 37°C, followed by 15 min. at 37°C in compound-free culture medium to complete de-esterification of the indicator. Ca²⁺ transients were imaged in individual cells under a confocal microscope, while perfusing hi-PSC-CMs (1 ml/min) at 37°C with physiological saline containing 140 mM NaCl, 4 mM KCl, 1 mM MgCl₂, 1.8 mM CaCl₂, 5 mM Glucose and 10 mM HEPES, pH 7.4 with NaOH, plus or minus 1 μ M Isoproterenol. Only spontaneously beating cells with regular frequency below 2 Hz were further selected for analysis. Data analysis was performed with in-house software, coded in the Interactive Data Language (IDL, Harris Geospatial Solutions). In each condition (baseline, Isoproterenol), statistical significance was assessed by unpaired 2-tailed t-tests with Welch correction for unequal variance (p < 0.05).

Statistical analysis

All data are presented as means \pm SEM. All datasets were analyzed for statistical significance by regular or repeated measures one-way ANOVA followed by Bonferroni's

post-test for multiple comparisons, or two-way ANOVA followed by Bonferroni's post-test (GraphPad Prism), as indicated in the figure legends. Survival curves were compared by the log-rank (Mantel-Cox) test. Differences were considered statistically significant at $p < 0.05$.

SUPPLEMENTAL TABLES

	Age				
	Neonates	3wk	5wk	2M	4M
LAX 2D LVEF (%)					
<i>WT</i>	46.02±16.11	49.60±16.94	48.37±4.56	53.04±8.36	54.99±6.89
<i>TMEM43WT</i>	54.83±6.10	55.75±5.75	49.88±5.01	59.41±3.95	58.64±8.46
<i>TMEM43mut</i>	45.03±13.65	43.42±8.11	44.58±14.83	43.70±2.57 ††	22.68±4.39 ***, †††, †††
LAX 2D LVEDV (µL)					
<i>WT</i>	4.43±0.83	38.97±4.92	49.07±9.66	49.48±18.68	57.58±3.93
<i>TMEM43WT</i>	4.93±2.17	46.61±7.92	54.51±6.46	61.42±11.34	60.77±13.10
<i>TMEM43mut</i>	3.55±0.66	39.36±5.76	45.82±9.99	68.11±7.25 **, †††	81.11±12.56 ***, †††, †††
APICAL 2D TAPSE (mm)					
<i>WT</i>	-	0.83±0.14	1.10±0.18	1.00±0.16	1.06±0.10
<i>TMEM43WT</i>	-	1.00±0.12	0.89±0.10	0.99±0.09	1.03±0.24
<i>TMEM43mut</i>	-	0.98±0.12	0.89±0.14	0.97±0.14	0.65±0.17 ***, †††, ††
RV FAC (%)					
<i>WT</i>	-	40.43±11.74	37.31±14.3	36.97±10.4	27.57±12.39
<i>TMEM43WT</i>	-	36.04±15.57	27.32±10.94	39.36±6.42	32.91±17.21
<i>TMEM43mut</i>	-	37.53±10.11	37.69±15.06	23.03±8.70	22.35±9.93
Heart-weight / body-weight (mg/g)					
<i>WT</i>	9.90±1.56	-	-	-	5.89±2.01
<i>TMEM43WT</i>	10.51±2.56	-	-	-	4.91±1.38
<i>TMEM43mut</i>	8.72±2.56	-	-	-	8.50±1.10 †
Lung-weight / body-weight (mg/g)					
<i>WT</i>	25.39±6.54	-	-	-	6.72±1.51
<i>TMEM43WT</i>	22.88±8.79	-	-	-	6.33±2.88
<i>TMEM43mut</i>	26.57±8.79	-	-	-	16.73±3.44 **, ††
Heart rate (bpm)					
<i>WT</i>	984.5±22.1	441.7±54.1†††	505.7±48.7†††	551.5±100.4†††	523.5±37.4†††
<i>TMEM43WT</i>	982.5±24.1	486.7±253.7†††	464.9±54.1†††	497.9±89.7†††	486.1±38.7†††
<i>TMEM43mut</i>	986.7±44.5	444.9±52.7†††	470.9±37.1†††	468.1±28.6†††	574.8±52.3†††

Supplemental Table 1. Echocardiography parameters related to systolic function, heart-weight to body weight ratios, and lung-weight to body-weight ratios in ARVC5 transgenic mice. LAX, long axis; 2D, two-dimensional mode; LVEF, left ventricular ejection fraction; LVEDV, left ventricular end-diastolic volume; TAPSE, tricuspid anterior systolic excursion; RV FAC, right ventricular fractional area change; bpm, beats per minute; WT, WT control mouse group; TMEM43WT, human

TMEM43WT-overexpressing mouse group; TMEM43mut, human TMEM43mut-overexpressing mouse group. Data are means \pm SD. ** $p < 0.01$, *** $p < 0.001$ compared with the WT group; † $p < 0.05$, †† $p < 0.01$, ††† $p < 0.001$ compared with the TMEM43WT group; ‡ $p < 0.01$ and ‡‡ $p < 0.001$ compared with neonates as the baseline time point. Echocardiography data were compared by two-way regular measures ANOVA with Bonferroni correction (except for TAPSE and RV FAC, in which repeated measures ANOVA was used). Heart-weight to body-weight and lung-weight to body-weight ratios were compared by one-way ANOVA with Bonferroni correction. $n=5-6$.

	Age				
	Neonates	3wk	5wk	2M	4M
p wave duration (ms)					
<i>WT</i>	11.87±0.81	11.83±2.36	10.75±1.20	10.41±0.60	9.18±0.53
<i>TMEM43WT</i>	11.28±0.78	10.10±1.54	10.75±0.47	9.67±0.35	9.90±0.71
<i>TMEM43mut</i>	11.33±0.49	11.32±1.43	12.54±0.47	14.62±0.54 ***, †††, \$\$\$	15.48±1.17 ***, †††, †††
QRS duration (ms)					
<i>WT</i>	10.78±1.77	10.27±0.66	11.05±1.04	10.59±0.66	10.23±0.56
<i>TMEM43WT</i>	11.15±0.39	10.16±0.42	11.19±0.96	11.15±0.61	10.61±0.67
<i>TMEM43mut</i>	11.08±1.13	9.98±1.43	11.08±0.71	10.56±0.86	14.29±1.28 ***, †††, †††
QRS amplitude (mV)					
<i>WT</i>	0.96±0.18	1.41±0.21	1.23±0.18	1.48±0.22	1.18±0.15
<i>TMEM43WT</i>	0.81±0.17	1.39±0.22	1.36±0.20	1.44±0.28	1.29±0.24
<i>TMEM43mut</i>	0.85±0.23	1.34±0.09	0.85±0.16 **, †††, †††	0.81±0.15 ***, †††, †††	0.38±0.10 ***, †††, †††

Supplemental Table 2. Electrocardiography parameters in *TMEM43mut* mice. p

wave, atrial depolarization; QRS complex, ventricular depolarization; WT, WT control mice; *TMEM43WT*, human *TMEM43WT*-overexpressing mice; *TMEM43mut*, human *TMEM43-S358L*-overexpressing mice. Data are presented as mean ±SD. ** $p < 0.01$, *** $p < 0.001$ compared with the WT group; ††† $p < 0.001$ compared with the *TMEM43WT* group; and ††† $p < 0.001$ compared with neonates as the baseline time point. Data were compared by two-way repeated measures ANOVA with Bonferroni correction, $n = 6$.

Supplemental Table 3. TMEM43 interacting proteins. P19 cells were transfected with expression plasmids for HA-tagged WT TMEM43 and TMEM43-S358L. WT and mutant TMEM43 were immunoprecipitated with an anti-HA antibody and the co-precipitating proteins were analyzed by quantitative proteomics. This is an online data set. Yellow, TMEM43-interacting protein identified; Red, protein-protein interaction that was lost in TMEM43-S358L; Blue, protein-protein interaction that was gained in TMEM43-S358L; Orange, TMEM43.

Supplemental Table 4. Transcriptional profile of different mouse lines. Wild type, TMEM43WT, and TMEM43mut mice were sacrificed at 2 months of age and the transcriptional profile was analyzed by RNA-Seq. This is an online data set.

Supplemental Table 5. Alternative splicing changes between TMEM43wt and WT mice and between TMEM43wt and TMEM43mut mice. "EVENT": Vast-tools event id. "GENE" Gene symbol of the gene in which the event is located. "TMEM43wt PSI": estimated percent spliced in (PSI) in the mice overexpressing the human WT TMEM43 protein; "WT PSI", PSI in WT mice; "TMEM43mut PSI": PSI in TMEM43mut mice. "dPSI", estimated difference in PSI between TMEM43wt and WT mice. " $P(|dPSI| > x) > 0.95$ ", difference in inclusion rate for which there is a 95% probability that the real absolute differences between genotypes is higher than that value. Only those alternative splicing events with values higher than 0, representing significantly changed events, are included.

4 Months	
LAX 2D LVEF (%)	
<i>WT</i>	54.99±6.89
<i>TMEM43mut</i>	22.69±4.39
<i>TMEM43mut-CnAβ1</i>	34.79±9.85^{***, †, ††}
LAX 2D LVEDV (μL)	
<i>WT</i>	57.58±3.93
<i>TMEM43mut</i>	81.11±12.56^{**}
<i>TMEM43mut-CnAβ1</i>	72.19±12.34
APICAL 2D TAPSE (mm)	
<i>WT</i>	1.06±0.10
<i>TMEM43mut</i>	0.65±0.17^{**}
<i>TMEM43mut-CnAβ1</i>	0.77±0.19^{††}
RV FAC (%)	
<i>WT</i>	27.57±12.39
<i>TMEM43mut</i>	22.35±9.93
<i>TMEM43mut-CnAβ1</i>	34.88±9.96
Heart-weight / body-weight (mg/g)	
<i>WT</i>	5.80±1.72
<i>TMEM43mut</i>	8.38±0.97^{**}
<i>TMEM43mut-CnAβ1</i>	5.13±0.87^{†††}
Lung-weight / body-weight (mg/g)	
<i>WT</i>	6.31±1.77
<i>TMEM43mut</i>	17.68±3.81^{***}
<i>TMEM43mut-CnAβ1</i>	7.81±0.82^{†††}
Heart rate (bpm)	
<i>WT</i>	523.5±37.4
<i>TMEM43mut</i>	574.8±52.31
<i>TMEM43mut-CnAβ1</i>	542.4±44.99

Supplemental Table 6. Echocardiography parameters related to systolic function, heart-weight to body weight ratios, and lung-weight to body-weight ratios in WT, *TMEM43mut*, and *TMEM43-CnAβ1* mice. LAX, long axis; 2D, two-dimensional mode; LVEF, left ventricular ejection fraction; LVEDV, left ventricular end-diastolic volume; TAPSE, tricuspid anterior systolic excursion; RV FAC, right ventricular fractional area change; bpm, beats per minute; WT, WT control mouse group; *TMEM43mut*, human

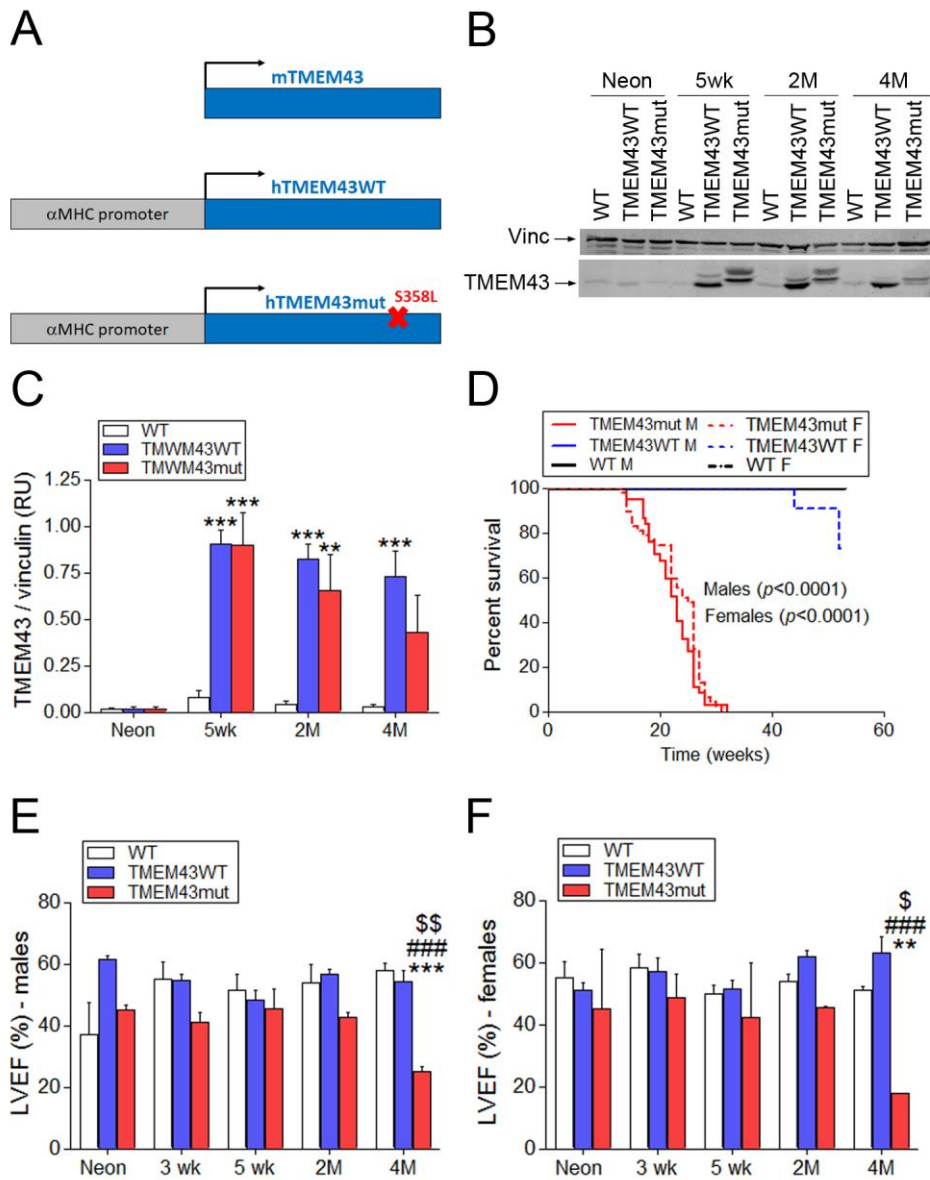
TMEM43mut-overexpressing mice group; TMEM43mut-CnA β 1, double transgenic mice overexpressing human TMEM43-S358L and CnA β 1. Data are means \pm SD. ** $p < 0.01$, *** $p < 0.001$ TMEM43mut compared with the WT group; † $p < 0.05$, †† $p < 0.001$ TMEM43-CnA β 1 compared with the TMEM43mut group, and ††† $p < 0.001$ TMEM43mut-CnA β 1 compared with WT. Data were compared by one-way ANOVA with Bonferroni correction, $n = 4-8$.

4 Months	
p wave (ms)	
<i>WT</i>	9.18±0.53
<i>TMEM43mut</i>	22.69±4.39
<i>TMEM43mut-CnAβ1</i>	34.79±9.85^{***,†,‡‡‡}
QRS duration (ms)	
<i>WT</i>	57.58±3.93
<i>TMEM43mut</i>	81.11±12.56^{**}
<i>TMEM43mut-CnAβ1</i>	72.19±12.34
QRS amplitude (mV)	
<i>WT</i>	1.06±0.10
<i>TMEM43mut</i>	0.65±0.17^{**}
<i>TMEM43mut-CnAβ1</i>	0.77±0.19^{‡‡‡}

Supplemental Table 7. Electrocardiography parameters in *TMEM43mut-CnAβ1*

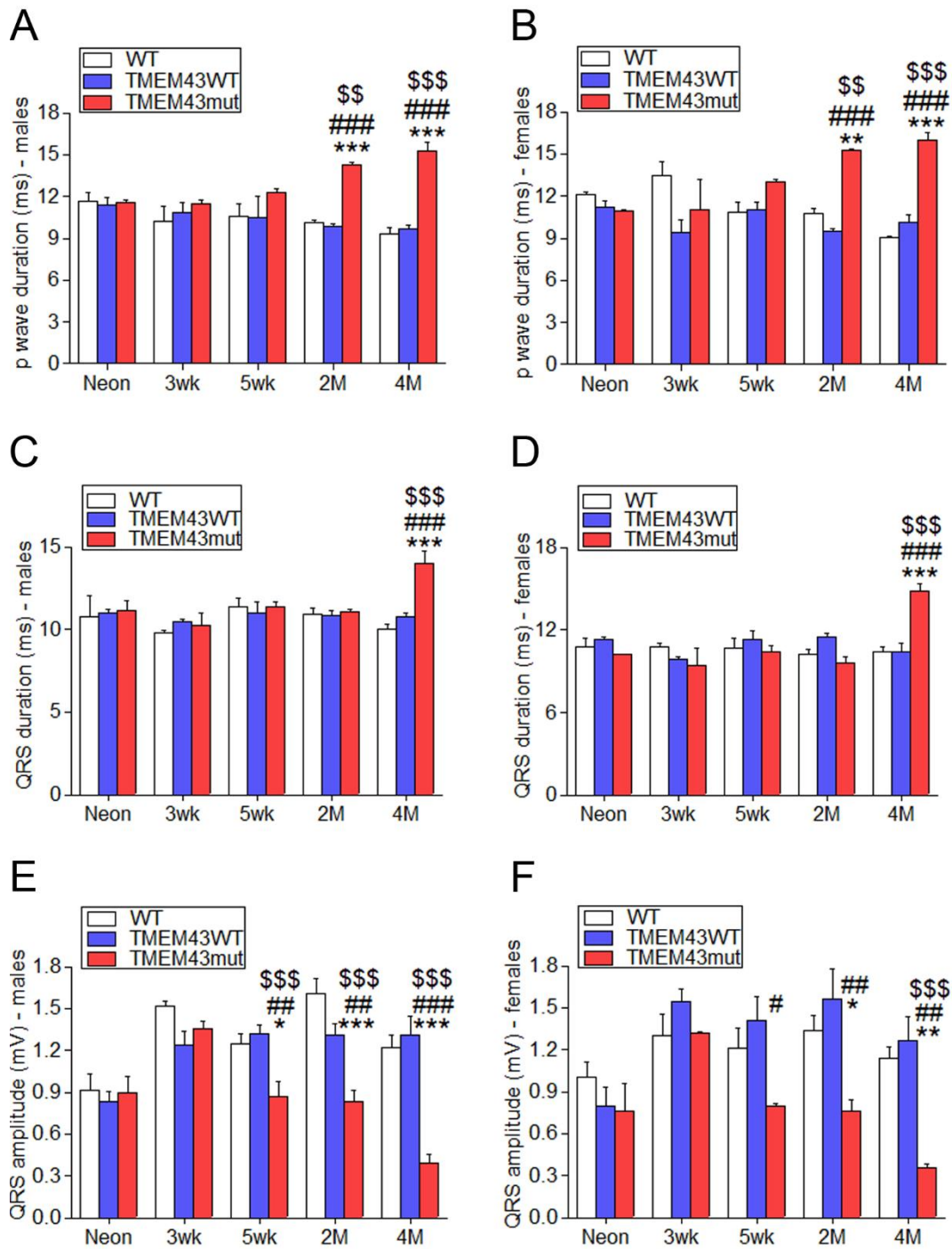
mice. p wave, atrial depolarization; QRS complex, ventricular depolarization; WT, WT control mice; *TMEM43mut*, human *TMEM43mut*-overexpressing mice; *TMEM43mut-CnAβ1*, double transgenic mice overexpressing human *TMEM43-S358L* and *CnAβ1*. Data are means ±SD. ^{**}*p*<0.01, ^{***}*p*<0.001 *TMEM43mut* compared with the WT group; [†]*p*<0.05 *TMEM43-CnAβ1* compared with the *TMEM43mut* group; and ^{‡‡‡}*p*<0.001 *TMEM43mut-CnAβ1* compared with WT. Data were compared by one-way ANOVA with Bonferroni correction, n=6.

SUPPLEMENTAL FIGURES



Supplemental Figure 1. Mouse lines used in this study and functional analysis of male and female mice. **A**, Three groups of mice were used: Wild type mice (top, WT), mice expressing the wild type version of human TMEM43 under the control of the alpha-mypsin heavy chain (α MHC) promoter (middle, hTMEM43WT) and mice expressing human TMEM43-S358L under the control of the α MHC promoter (bottom, hTMEM43mut). **B**, **C**, TMEM43 expression was analyzed at different time points in the three mouse lines by western blot (**B**) and quantified (**C**). Vinc, vinculin **D**, Male (n=66) and Female (n=74) were monitored for 60 weeks and their survival rate determined from a Kaplan-Meier curve. The indicated p-value was obtained with a log-rank test. **E**, **F**, Left

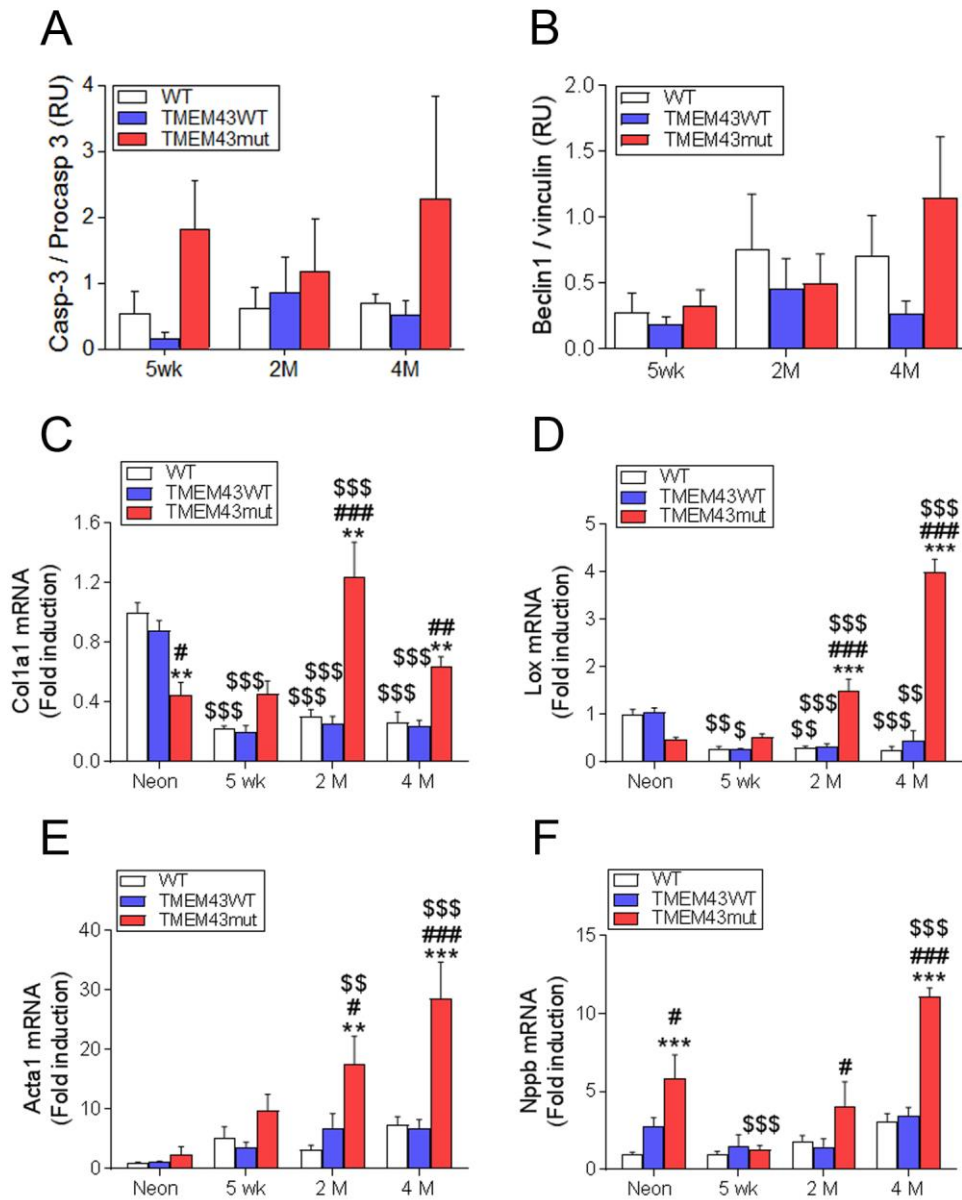
ventricular ejection fraction (LVEF) was assessed by echocardiography at birth (Neon.) and at 3 and 5 weeks and 2 and 4 months of age in male (**E**) and female mice (**F**). Graphs show mean \pm SEM. ** $p < 0.01$, *** $p < 0.001$ TMEM43mut vs WT; ### $p < 0.001$ TMEM43mut vs TMEM43WT; \$ $p < 0.05$, \$\$ $p < 0.01$ for different time points vs neonates for each mouse line; two-way ANOVA followed by Bonferroni's post-test, $n = 5-6$ per group.



Supplemental Figure 2. Electrocardiography analysis of male and female mice. A-

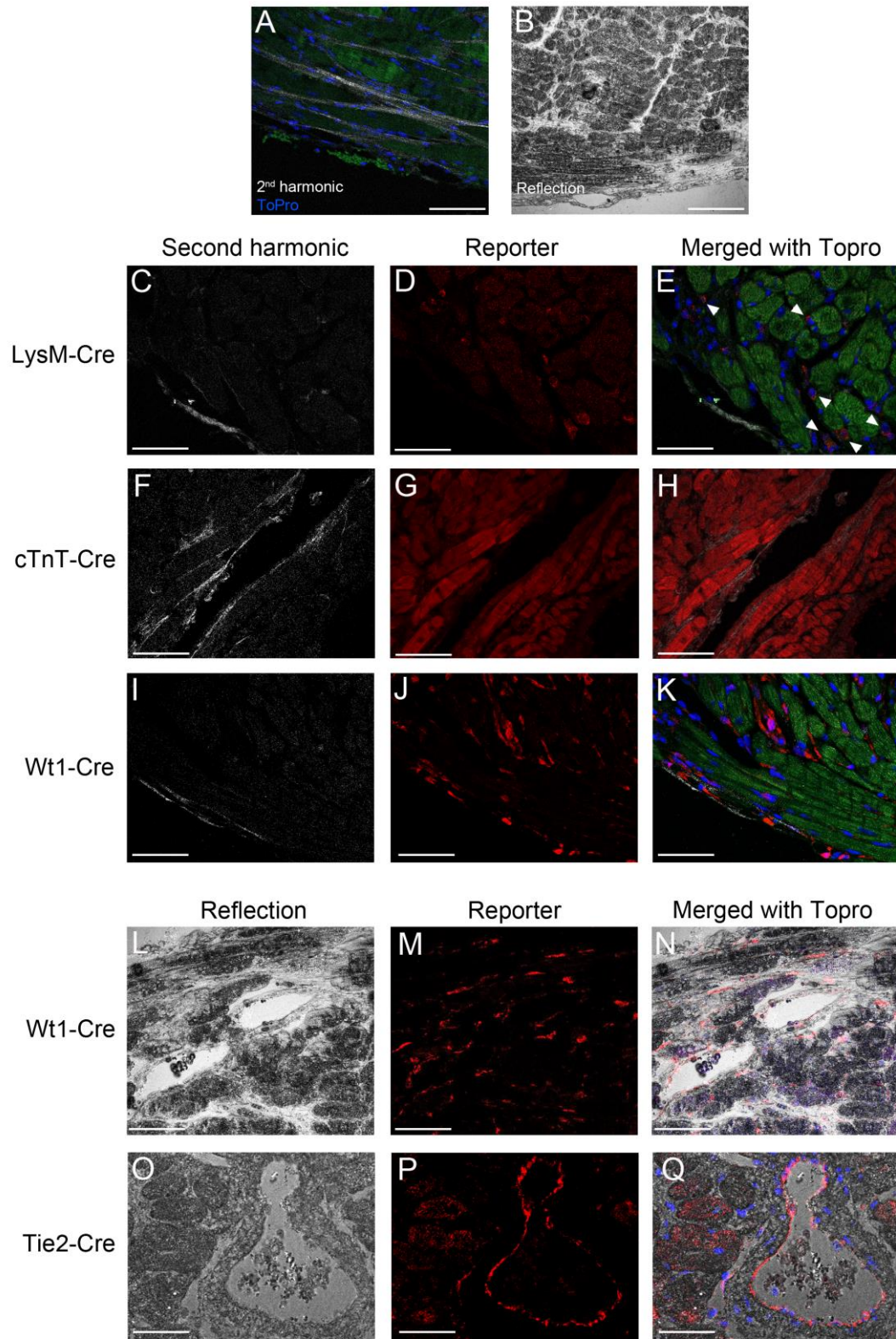
F, p-wave duration (**A, B**) and QRS duration and amplitude (**C-F**) were assessed at birth (Neon.) and at 3 and 5 weeks and 2 and 4 months of age in male and female WT, TMEM43WT and TMEM43mut mice. Graphs show mean \pm SEM. * $p < 0.05$, ** $p < 0.01$, *** $p < 0.001$ TMEM43mut vs WT; # $p < 0.05$, ## $p < 0.01$, ### $p < 0.001$ TMEM43mut vs TMEM43WT

TMEM43WT; $^{**}p < 0.01$, $^{***}p < 0.001$ for different time points vs neonates for each mouse line; two-way repeated measures ANOVA followed by Bonferroni's post-test, $n=6$.



Supplemental Figure 3. TMEM43-S358L increases cell death and the expression of fibrosis and cardiac dysfunction markers. A-B Activated caspase-3 (casp-3, **A**) and beclin1 (**B**) quantified in the different mice at 5 weeks, 2 and 4 months of age; n=3-5. **C-F**, qRT-PCR analysis of the expression of collagen I α 1 (Col1a1; **C**), lysyl oxidase (Lox; **D**), α -skeletal actin (Acta1; **E**) and brain natriuretic peptide (BNP/Nppb; **F**) in myocardial RNA isolated at the indicated ages. Graphs show data points for individual mice and mean \pm SEM. **p<0.01, ***p<0.001 TMEM43mut vs WT; #p<0.05, ##p<0.01, ###p<0.001 TMEM43mut vs TMEM43WT; \$p<0.05, \$\$p<0.01, \$\$\$p<0.001 for different ages vs

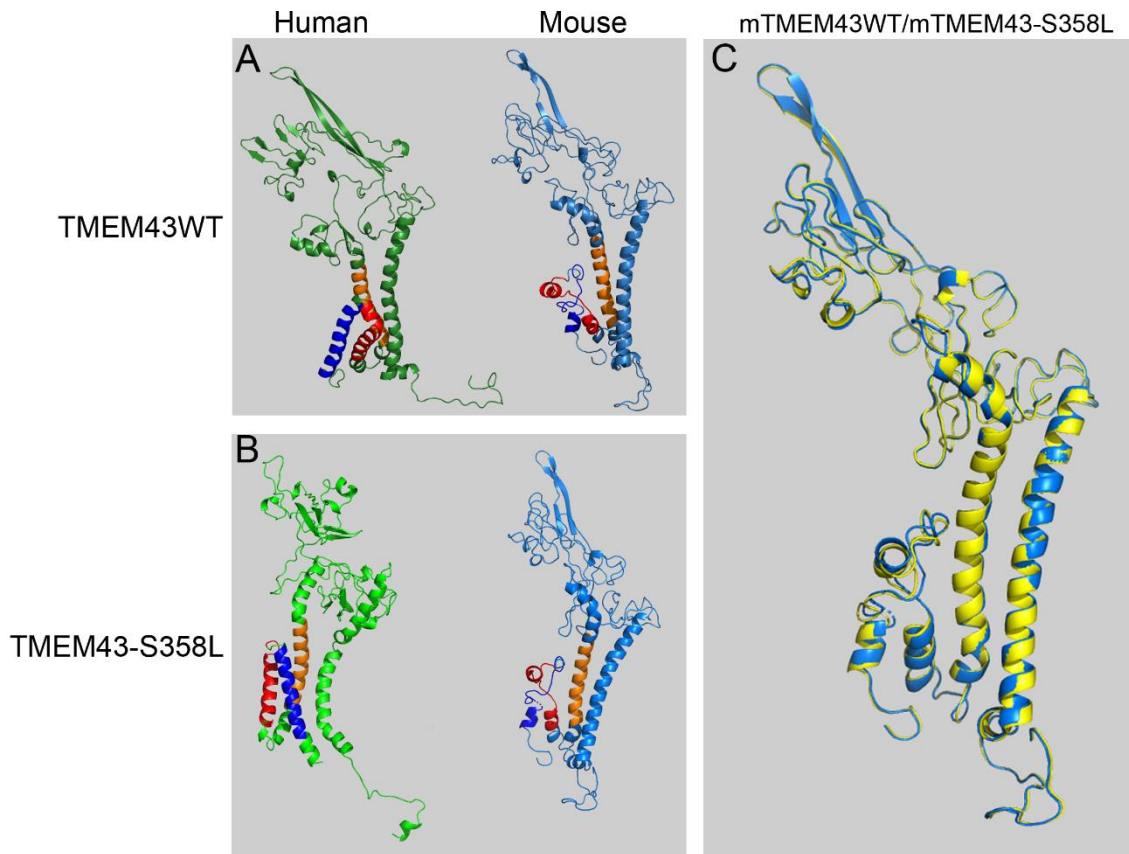
neonates for each mouse line; two-way ANOVA followed by Bonferroni's post-test; n=18-29.



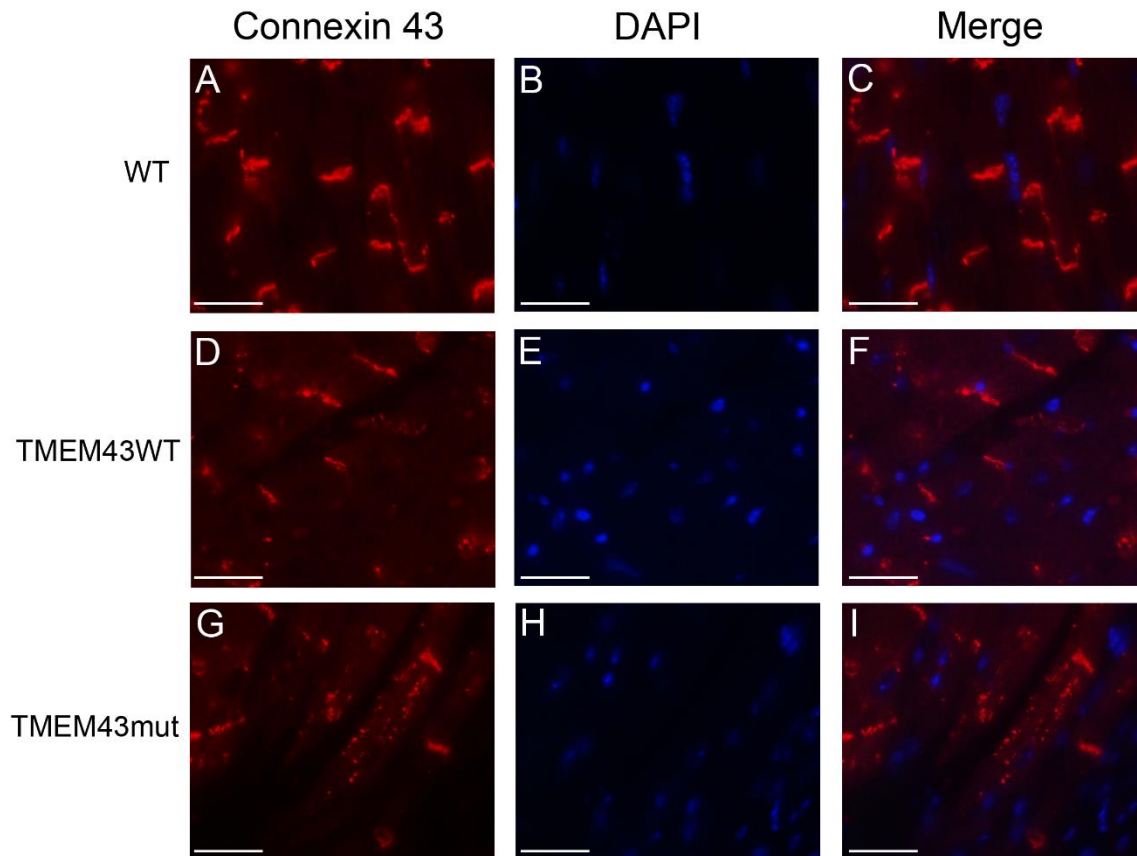
Supplemental Figure 4. Epicardium-derived cells contribute to fibrosis in ARVC5.

A, B, *TMEM43*^{mut} mice were crossed with reporter mice in which the expression of the reporter protein is induced upon removal of the preceding STOP codon by the Cre

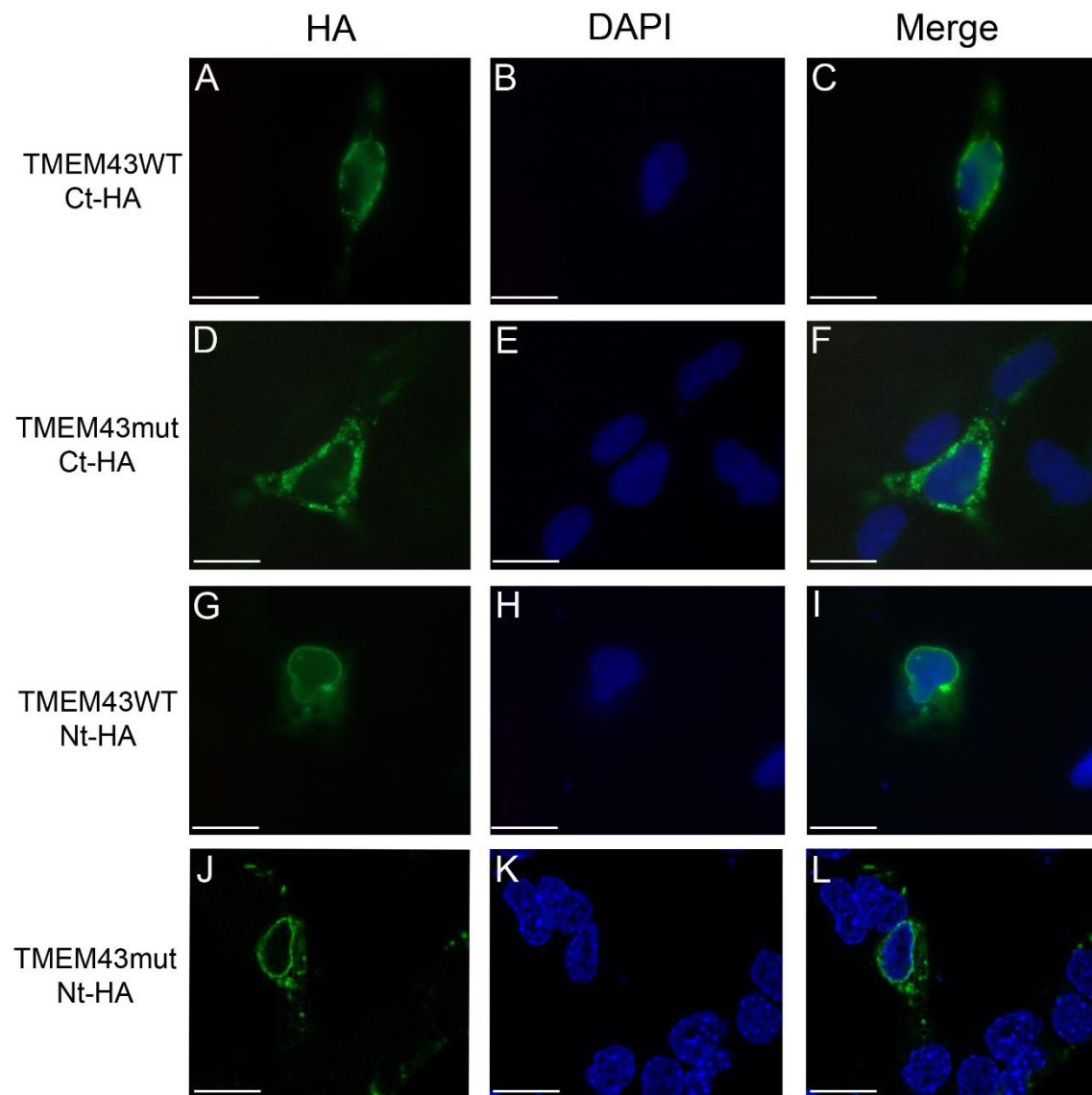
recombinase. The presence of organized mature collagen fibers was determined in myocardial sections at 4 months of age by second harmonic generation microscopy (A, white) and total collagen fibers were detected by reflection microscopy (B, white). C-K, lysozyme M (LysM)-Cre labeled macrophages (C-E), cardiac troponin T (cTnT)-labeled cardiomyocytes (F-H), Wilms tumor (Wt1)-Cre epicardium-derived cells (I-N) and Tie2-Cre derived endothelium (O-Q). Only colocalization of the Wt1 reporter signal can be observed close to or within collagen fibers (I-N). White arrowheads in E indicate reporter-positive cells. Bar, 50 μ m.



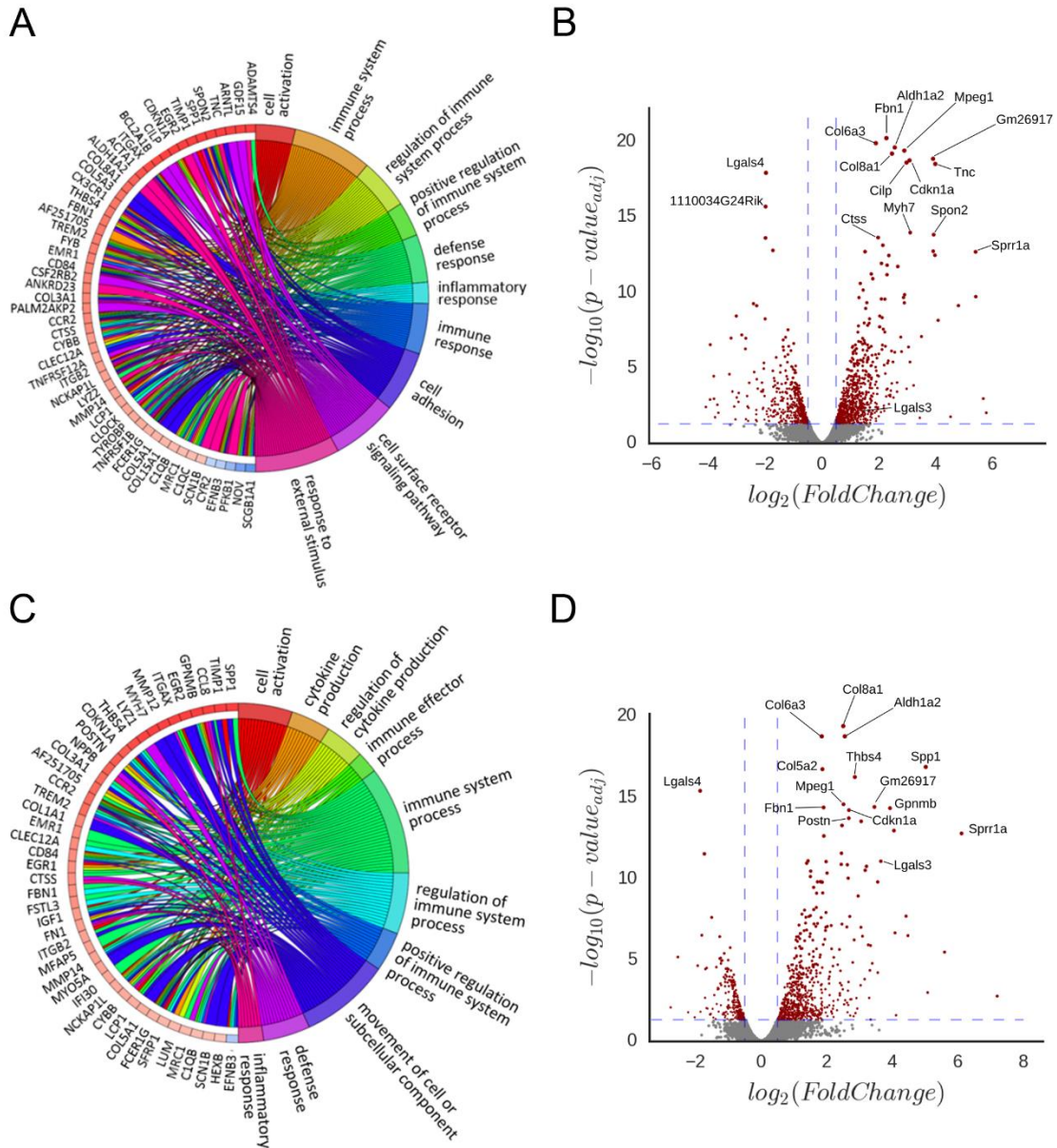
Supplemental Figure 5. The S358L mutation alters TMEM43 conformation and protein interactions. A-F, *In silico* modeling of the tertiary structure of WT (A) and mutant TMEM43 (B) as monomers in human (green) and mouse (blue). Orange, transmembrane domain 1 (TM1); red, TM3; dark blue, TM4. C, Superimposed tertiary structures of WT and mutant TMEM43 mouse proteins. Blue molecule, mouse WT TMEM43; yellow molecule, mouse mutant TMEM43.



Supplemental Figure 6. A-I, Connexin 43 distribution in the different mouse lines. Connexin 43 distribution was analyzed by immunofluorescence in wild type (WT) (**A-C**), TMEM43WT (**D-F**), and TMEM43mut mice (**G-I**). Nuclei were counterstained with DAPI. Bar, 50 μ m.



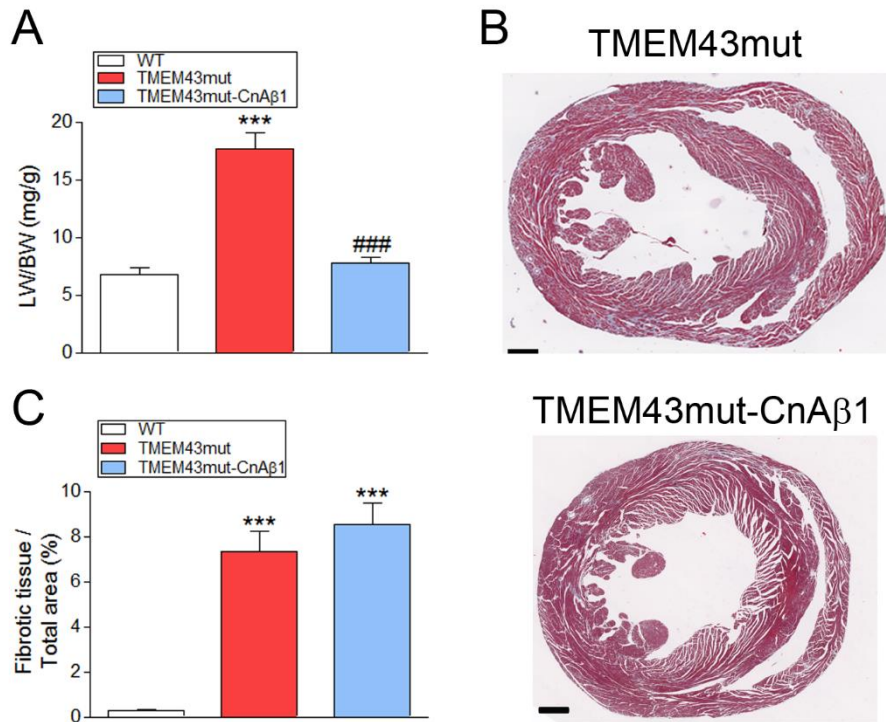
Supplemental Figure 7. Intracellular localization of TMEM43. A-L, P19 cells were transfected with different HA-tagged TMEM43 constructs. The intracellular localization of TMEM43 in each case was determined by anti-HA immunofluorescence. Nuclei were counterstained with DAPI. Bar, 10 μ m.



Supplemental Figure 8. Expression of TMEM43-S358L is associated with genes involved in the immune response and fibrosis. A-D, Differential gene expression results for the contrasts TMEM43mut mice vs WT mice (**A**, **B**) and for TMEM43mut vs TMEM43WT (**C**, **D**), were visualized using GoChord plots (**A**, **C**) and volcano plots (**B**, **D**). Volcano plots show the estimated change in expression levels presented as the log of the fold change between the two conditions on the x-axis, and the significance of each gene, represented as the $-\log$ transformation of the adjusted p-value on the y-axis.

Genes found to be differentially expressed in a significant manner are highlighted in red.

Among them, we added labels for some of the most up- or down-regulated genes.



Supplemental Figure 9. CnAβ1 reduces pulmonary congestion and ventricular dilatation. **A**, Lung-weight to body-weight ratio (LW/BW) in 4-month-old WT, TMEM43mut and TMEM43mut-CnAβ1 mice. **B**, Cardiac cross-sections of representative TMEM43mut and TMEM43mut-CnAβ1 mouse hearts stained with Masson’s trichrome protocol. Bar, 50 μm. **C**, Percentage fibrotic area in the three mouse lines. Graphs show data points for individual mice and mean ±SEM. ***p<0.001 vs WT mice; ###p<0.001 TMEM43mut-CnAβ1 mice vs TMEM43mut mice, 1-way ANOVA with Bonferroni correction n=4-8 (A); n=18 per group (C). Note that WT and TMEM43mut mice data for (A) and (C) are those shown in Fig. 1H and 3I, respectively, and are repeated here for comparative purposes.

SUPPLEMENTAL VIDEOS

Supplemental Video 1. Long axis echocardiography of hearts from wild type (WT), TMEM43WT and TMEM43mut mice at 4 months of age.

Supplemental Video 2. Long axis echocardiography of hearts from wild type (WT), TMEM43mut and TMEM43mut-CnA β 1 mice at 4 months of age.

SUPPLEMENTAL BIBLIOGRAPHY

1. Felkin LE, Narita T, Germack R, Shintani Y, Takahashi K, Sarathchandra P, López-Olañeta MM, Gómez-Salineró JM, Suzuki K, Barton PJR, et al. Calcineurin splicing variant CnA β 1 improves cardiac function after myocardial infarction without inducing hypertrophy. *Circulation*. 2011;123:2838-2847.
2. Kisanuki YY, Hammer RE, Miyazaki J, Williams SC, Richardson JA, Yanagisawa M. Tie2-cre transgenic mice: A new model for endothelial cell-lineage analysis in vivo. *Dev. Biol.* 2001;230:230-242.
3. Clausen BE, Burkhardt C, Reith W, Renkawitz R, Frster I. Conditional gene targeting in macrophages and granulocytes using lysmcre mice. *Transgenic Res.* 1999;8:265-277.
4. del Monte G, Casanova JC, Guadix JA, MacGrogan D, Burch JBE, Pérez-Pomares JM, de la Pompa JL. Differential Notch signaling in the epicardium is required for cardiac inflow development and coronary vessel morphogenesis. *Circ. Res.* 2011;108:824-836.
5. Jiao K, Kulesa H, Tompkins K, Zhou Y, Batts L, Baldwin HS, Hogan BLM. An essential role of bmp4 in the atrioventricular septation of the mouse heart. *Genes Dev.* 2003;17:2362-2367.
6. Reiser K, Stoller P, Knoesen A. Three-dimensional geometry of collagenous tissues by second harmonic polarimetry. *Sci. Rep.* 2017;7:2642.
7. Whittaker P, Kloner RA, Boughner DR, Pickering JG. Quantitative assessment of myocardial collagen with picosirius red staining and circularly polarized light. *Basic Res. Cardiol.* 1994;89:397-410.
8. de Jong S, van Veen TAB, de Bakker JMT, van Rijen HVM. Monitoring cardiac fibrosis: A technical challenge. *Neth. Heart J.* 2012;20:44-48.
9. Schindelin J, Arganda-Carreras I, Frise E, Kaynig V, Longair M, Pietzsch T, Preibisch S, Rueden C, Saalfeld S, Schmid B, et al. Fiji: An open-source platform for biological-image analysis. *Nat. Meth.* 2012;9:676.
10. Villarroya-Beltri C, Gutiérrez-Vázquez C, Sánchez-Cabo F, Pérez-Hernández D, Vázquez J, Martín-Cofreces N, Martínez-Herrera DJ, Pascual-Montano A, Mittelbrunn M, Sánchez-Madrid F. Sumoylated hnRNP A2b1 controls the sorting of miRNAs into exosomes through binding to specific motifs. *Nat. Commun.* 2013;4:2980.
11. Ruijter JM, Ramakers C, Hoogaars WMH, Karlen Y, Bakker O, van den Hoff MJB, Moorman AFM. Amplification efficiency: Linking baseline and bias in the analysis of quantitative pcr data. *Nucleic Acids Res.* 2009;37:e45.
12. Walter W, Sánchez-Cabo F, Ricote M. Gplot: An r package for visually combining expression data with functional analysis. *Bioinformatics.* 2015;31:2912-2914.
13. Tapial J, Ha KCH, Sterne-Weiler T, Gohr A, Braunschweig U, Hermoso-Pulido A, Quesnel-Vallièrès M, Permanyer J, Sodaei R, Marquez Y, et al. An atlas of alternative splicing profiles and functional associations reveals new regulatory programs and genes that simultaneously express multiple major isoforms. *Genome Res.* 2017;27:1759-1768.
14. Irimia M, Weatheritt Robert J, Ellis JD, Parikshak Neelroop N, Gonatopoulos-Pournatzis T, Babor M, Quesnel-Vallièrès M, Tapial J, Raj B, O'Hanlon D, et al. A highly conserved program of neuronal microexons is misregulated in autistic brains. *Cell.* 2014;159:1511-1523.
15. Han H, Braunschweig U, Gonatopoulos-Pournatzis T, Weatheritt RJ, Hirsch CL, Ha KCH, Radovani E, Nabeel-Shah S, Sterne-Weiler T, Wang J, et al. Multilayered control of alternative splicing regulatory networks by transcription factors. *Mol. Cell.* 2017;65:539-553.e537.

16. Barth P, Wallner B, Baker D. Prediction of membrane protein structures with complex topologies using limited constraints. *Proc. Natl. Acad. Sci. U S A.* 2009;106:1409-1414.
17. Yang J, Yan R, Roy A, Xu D, Poisson J, Zhang Y. The i-tasser suite: Protein structure and function prediction. *Nat. Meth.* 2015;12:7-8.
18. Alford RFa. An integrated framework advancing membrane protein modeling and design. *PLoS Comput. Biol.* 2015;11:e1004398.
19. Lian X, Zhang J, Azarin SM, Zhu K, Hazeltine LB, Bao X, Hsiao C, Kamp TJ, Palecek SP. Directed cardiomyocyte differentiation from human pluripotent stem cells by modulating wnt/ β -catenin signaling under fully defined conditions. *Nat. Protoc.* 2012;8:162.
20. da Rocha AM, Campbell K, Mironov S, Jiang J, Mundada L, Guerrero-Serna G, Jalife J, Herron TJ. Hipsc-cm monolayer maturation state determines drug responsiveness in high throughput pro-arrhythmia screen. *Sci. Rep.* 2017;7:13834.
21. Sala L, Meer BJv, Tertoolen LGJ, Bakkers J, Bellin M, Davis RP, Denning C, Dieben MAE, Eschenhagen T, Giacomelli E, et al. Musclemotion. *Circ. Res.* 2018;122:e5-e16.